Supplementary Information

ssDNA-amphiphile architecture used to control dimensions of DNA nanotubes

Huihui Kuang,[a] Thomas E. Gartner III,[b] Matheus Dorneles de Mello,[c] Jun Guo,[a] Xiaobing Zuo,[d] Michael Tsapatsis,[a,e] Arthi Jayaraman[b,f] and Efrosini Kokkoli*[a,e]

[a] Institute for NanoBioTechnology, Johns Hopkins University, Baltimore, MD 21218, USA. E-mail: kokkoli@jhu.edu

[b] Department of Chemical and Biomolecular Engineering, University of Delaware, Newark, DE 19716, USA.

[c] Department of Chemical Engineering and Materials Science, University of Minnesota, Minneapolis, MN 55455, USA.

[d] X-Ray Science Division, Argonne National Laboratory, Argonne, IL 60439, USA.

[e] Department of Chemical and Biomolecular Engineering, Johns Hopkins University, Baltimore, MD 21218, USA.

[f] Department of Materials Science and Engineering, University of Delaware, Newark, DE 19716, USA.

Experimental

Synthesis of hydrophobic tails

Dialkyl tails with different lengths (C_{16}, C_{18} or C_{20}) were synthesized as depicted in Fig. S1. Glutamic acid and *p*-toluenesulfonate (1.2x molar excess) were first mixed in toluene and refluxed for 1 h at 130 °C. Then hexadecanol (C_{16}), octadecanol (C_{18}), or eicosanol (C_{20}) at 2.2x molar excess was added. The mixture was heated until an equimolar amount of water was recovered in a Dean-Stark trap. The toluene was removed and product **1** recrystallized from acetone three times. **1** was dissolved in $CHCl_3$/THF (50/50%, v/v) at 50 °C, and 15% molar excess of succinic anhydride and 50% molar excess of *N,N*-diisopropylethylamine (DIEA) were added. After 6 h the solvents were evaporated and product **2** was recrystallized from ethyl acetate. *N*-hydroxysuccinimide (NHS, 1.5x molar excess) was added to a solution of **2** in dichloromethane (DCM) at room temperature. After cooling to 0 °C, *N,N′*-dicyclohexylcarbodiimide (DCC, 2x molar excess) was added. The solution was stirred for 1 h at 0 °C and then overnight at room temperature. The precipitated dicyclohexyl urea (DCU) was filtered off, and solvent was removed in vacuum. Product **3** was recrystallized from ethyl acetate. The NHS-activated **3** was then reacted with 1.5x molar excess of 12-aminododecanoic acid in methanol for 6 h at 50 °C. Then methanol was removed, and DCM was added to dissolve product **4**. The excess 12-aminododecanoic acid that didn't dissolve in DCM was removed by filtration. DCM was then evaporated and product **4** was recrystallized from ethyl acetate. NHS (1.5x molar excess) was added to a solution of **4** in DCM at room temperature. After cooling to 0 °C, DCC (2x molar excess) was added. The solution was stirred for 1 h at 0 °C and then overnight at room temperature. The precipitated DCU was filtered off, and solvent was removed in vacuum. Product **5** was recrystallized from ethyl acetate. ^{1}H NMR spectra were recorded on a Varian Inova 300 MHz spectrometer with deuterated chloroform ($CDCl_3$) as a solvent at room temperature. Proton chemical shifts were referenced to tetramethyl silane (TMS) (0.00 ppm, in $CDCl_3$). ESI-MS was recorded with a Bruker BioTOF II instrument in positive ion mode for NHS-activated compounds.

Products **1**-**5** were characterized with ^{1}H NMR (300 MHz, $CDCl_3$) δ (ppm):
(**1a**): 0.88 (t, 6H, -C*H*$_3$), 1.25 (m, 52H, -C*H*$_2$-), 1.54 (m, 4H, -C*H*$_2$CH-OCO), 2.18 (tt, 2H, -COCH$_2$C*H*$_2$CHCO, NH), 2.34 (s, 3H, -C$_6$H$_4$C*H*$_3$), 2.45 (h, 2H, -COC*H*$_2$CH$_2$-), 4.00 (tt, 4H, -C*H*$_2$OCO-), 7.76,7.72,7.14,7.10 (dd, 4, -OSO$_3$C$_6$*H*$_4$CH$_3$), 8.29 (b, 3 H, -N*H*$_3^+$- OSO$_3$-).

(**1b**): 0.88 (t, 6H, -C*H*$_3$), 1.25 (m, 60H, -C*H*$_2$-), 1.54 (m, 4H, -C*H*$_2$CH-OCO), 2.18 (tt, 2H, -COCH$_2$C*H*$_2$CHCO, NH), 2.34 (s, 3H, -C$_6$H$_4$C*H*$_3$), 2.45 (h, 2H, -COC*H*$_2$CH$_2$-), 4.00 (tt, 4H, -C*H*$_2$OCO-), 7.76,7.72,7.14,7.10 (dd, 4, -OSO$_3$C$_6$*H*$_4$CH$_3$), 8.29 (b, 3 H, -N*H*$_3^+$- OSO$_3$-).

(**1c**): 0.88 (t, 6H, -C*H*$_3$), 1.25 (m, 68H, -C*H*$_2$-), 1.54 (m, 4H, -C*H*$_2$CH-OCO), 2.18 (tt, 2H, -COCH$_2$C*H*$_2$CHCO, NH), 2.34 (s, 3H, -C$_6$H$_4$C*H*$_3$), 2.45 (h, 2H, -COC*H*$_2$CH$_2$-), 4.00 (tt, 4H, -C*H*$_2$OCO-), 7.76,7.72,7.14,7.10 (dd, 4, -OSO$_3$C$_6$*H*$_4$CH$_3$), 8.29 (b, 3 H, -N*H*$_3^+$- OSO$_3$-).

(**2a**): 0.88 (t, 6H, -C*H*$_3$), 1.25 (m, 52H, C*H*$_2$), 1.61 (m, 4H, -C*H*$_2$CH$_2$-OCO), 1.91, 2.09 (tt, 2H, -COCH$_2$C*H*$_2$CHCO, NH), 2.25 (h, 2H, -COC*H*$_2$CH$_2$-), 2.56, 2.59 (tt, 4H, NHCOC*H*$_2$C*H*$_2$COOH), 4.00 (tt, 4H, -C*H*$_2$OCO), 4.59 (tt, 1, CH$_2$C*H*CO, NH), 6.37 (d, 1H, OCOCHN*H*CO-).

(**2b**): 0.88 (t, 6H, -C*H*$_3$), 1.25 (m, 60H, C*H*$_2$), 1.61 (m, 4H, -C*H*$_2$CH$_2$-OCO), 1.91, 2.09 (tt, 2H, -COCH$_2$C*H*$_2$CHCO, NH), 2.25 (h, 2H, -COC*H*$_2$CH$_2$-), 2.56, 2.59 (tt, 4H, NHCOC*H*$_2$C*H*$_2$COOH), 4.00 (tt, 4H, -C*H*$_2$OCO), 4.59 (tt, 1, CH$_2$C*H*CO,NH), 6.37 (d, 1H, OCOCHN*H*CO-).

(**2c**): 0.88 (t, 6H, -C*H*$_3$), 1.25 (m, 68H, C*H*$_2$), 1.61 (m, 4H, -C*H*$_2$CH$_2$-OCO), 1.91, 2.09 (tt, 2H, -COCH$_2$C*H*$_2$CHCO, NH), 2.25 (h, 2H, -COC*H*$_2$CH$_2$-), 2.56, 2.59 (tt, 4H, NHCOC*H*$_2$C*H*$_2$COOH), 4.00 (tt, 4H, -C*H*$_2$OCO), 4.59 (tt, 1, CH$_2$C*H*CO, NH), 6.37 (d, 1H, OCOCHN*H*CO-).

(**3a**): 0.88 (t, 6H, -C*H*$_3$), 1.25 (m, 52H, C*H*$_2$), 1.61 (m, 4H, -C*H*$_2$CH$_2$-OCO), 1.91, 2.09 (tt, 2H, -COCH$_2$C*H*$_2$CHCO, NH), 2.25 (h, 2H, -COC*H*$_2$CH$_2$-), 2.66 (tt, 2H, NHCOC*H*$_2$CH$_2$COO-), 2.84 (tt, 4H, -NCOC*H*$_2$C*H*$_2$CO-), 2.99 (tt, 2H, NHCOCH$_2$C*H*$_2$COO-), 4.00 (tt, 4H, -C*H*$_2$OCO), 4.59 (tt, 1, CH$_2$C*H*CO, NH), 6.37 (d, 1H, OCOCHN*H*CO-).

(**3b**): 0.88 (t, 6H, -C*H*$_3$), 1.25 (m, 60H, C*H*$_2$), 1.61 (m, 4H, -C*H*$_2$CH$_2$-OCO), 1.91, 2.09 (tt, 2H, -COCH$_2$C*H*$_2$CHCO, NH), 2.25 (h, 2H, -COC*H*$_2$CH$_2$-), 2.66 (tt, 2H, NHCOC*H*$_2$CH$_2$COO-), 2.84 (tt, 4H, -NCOC*H*$_2$C*H*$_2$CO-), 2.99 (tt, 2H, NHCOCH$_2$C*H*$_2$COO-), 4.00 (tt, 4H, -C*H*$_2$OCO), 4.59 (tt, 1, CH$_2$C*H*CO, NH), 6.37 (d, 1H, OCOCHN*H*CO-).

(**3c**): 0.88 (t, 6H, -C*H*$_3$), 1.25 (m, 68H, C*H*$_2$), 1.61 (m, 4H, -C*H*$_2$CH$_2$-OCO), 1.91, 2.09 (tt, 2H, -COCH$_2$C*H*$_2$CHCO, NH), 2.25 (h, 2H, -COC*H*$_2$CH$_2$-), 2.66 (tt, 2H, NHCOC*H*$_2$CH$_2$COO-), 2.84 (tt, 4H, -NCOC*H*$_2$C*H*$_2$CO-), 2.99 (tt, 2H, NHCOCH$_2$C*H*$_2$COO-), 4.00 (tt, 4H, -C*H*$_2$OCO), 4.59 (tt, 1, CH$_2$C*H*CO, NH), 6.37 (d, 1H, OCOCHN*H*CO-).

(**4a**): 0.88 (t, 6H, -C*H*$_3$), 1.25 (m, 66H, C*H*$_2$), 1.47 (m, 2H, -CH$_2$C*H*$_2$CH$_2$), 1.61 (m, 6H, -C*H*$_2$CH$_2$-OCO, -C*H*$_2$CH$_2$COOH), 1.91, 2.09 (tt, 2H, -COCH$_2$C*H*$_2$CHCO, NH), 2.25 (h, 2H, -COC*H*$_2$CH$_2$-), 2.56, 2.59 (t, 4H, NHCOC*H*$_2$C*H*$_2$COOH), 2.96 (tt, 2H, -C*H*$_2$OCOH), 3.21(m, 2H, -NHC*H*$_2$CH$_2$),), 4.00 (tt, 4H, -C*H*$_2$OCO), 4.59 (tt, 1, CH$_2$C*H*CO, NH), 6.11 (t, 1H, OCN*H*CH$_2$-), 6.78 (d, 1H, OCOCHN*H*CO-).

(**4b**): 0.88 (t, 6H, -C*H*$_3$), 1.25 (m, 74H, C*H*$_2$), 1.47 (m, 2H, -CH$_2$C*H*$_2$CH$_2$), 1.61 (m, 6H, -C*H*$_2$CH$_2$-OCO, -C*H*$_2$CH$_2$COOH), 1.91, 2.09 (tt, 2H, -COCH$_2$C*H*$_2$CHCO, NH), 2.25 (h, 2H, -COC*H*$_2$CH$_2$-), 2.56, 2.59 (tt, 4H, NHCOC*H*$_2$C*H*$_2$COOH), 2.96 (tt, 2H, -C*H*$_2$OCOH), 3.21(tt, 2H, -NHC*H*$_2$CH$_2$),), 4.00 (tt, 4H, -C*H*$_2$OCO), 4.59 (tt, 1, CH$_2$C*H*CO,NH), 6.11 (t, 1H, OCN*H*CH$_2$-), 6.78 (d, 1H, OCOCHN*H*CO-).

(**4c**): 0.88 (t, 6H, -C*H*$_3$), 1.25 (m, 82H, C*H*$_2$), 1.47 (m, 2H, -CH$_2$C*H*$_2$CH$_2$), 1.61 (m, 6H, -C*H*$_2$CH$_2$-OCO, -C*H*$_2$CH$_2$COOH), 1.91, 2.09 (tt, 2H, -COCH$_2$C*H*$_2$CHCO, NH), 2.25 (h, 2H, -COC*H*$_2$CH$_2$-), 2.56, 2.59 (tt, 4H, NHCOC*H*$_2$C*H*$_2$COOH), 2.96 (tt, 2H, -C*H*$_2$OCOH), 3.21(tt, 2H, -NHC*H*$_2$CH$_2$),), 4.00 (tt, 4H, -C*H*$_2$OCO), 4.59 (tt, 1, CH$_2$C*H*CO, NH), 6.11 (t, 1H, OCN*H*CH$_2$-), 6.78 (d, 1H, OCOCHN*H*CO-).

(**5a**): 0.88 (t, 6H, -C*H*$_3$), 1.25 (m, 66H, C*H*$_2$), 1.47 (m, 2H, -NHCH$_2$C*H*$_2$CH$_2$), 1.61 (m, 6H, -C*H*$_2$CH$_2$-OCO, -C*H*$_2$CH$_2$COO-), 1.91, 2.09 (tt, 2H, -COCH$_2$C*H*$_2$CHCO, NH), 2.35 (h, 2H, -COC*H*$_2$CH$_2$-), 2.50 (tt, 2H, NHCOC*H*$_2$CH$_2$COO-), 2.55 (tt, 4H, NHCOCH$_2$C*H*$_2$COO-, -C*H*$_2$OCO-), 2.84 (tt, 4H, -NCOC*H*$_2$C*H*$_2$CO-), 3.20 (tt, 2H, -NHC*H*$_2$CH$_2$-), 4.00 (tt, 4H, -C*H*$_2$OCO), 4.59 (tt, 1, CH$_2$C*H*CO, NH), 5.87 (t, 1H, OCN*H*CH$_2$-), 6.62 (d, 1H, OCOCHN*H*CO-). ESI-MS: [M +Na]$^+$ 1012.7.

(**5b**): 0.88 (t, 6H, -C*H*$_3$), 1.25 (m, 74H, C*H*$_2$), 1.47 (m, 2H, -NHCH$_2$C*H*$_2$CH$_2$), 1.61 (m, 6H, -C*H*$_2$CH$_2$-OCO, -C*H*$_2$CH$_2$COO-), 1.91, 2.09 (tt, 2H, -COCH$_2$C*H*$_2$CHCO, NH), 2.35 (h, 2H, -COC*H*$_2$CH$_2$-), 2.50 (tt, 2H, NHCOC*H*$_2$CH$_2$COO-), 2.55 (tt, 4H, NHCOCH$_2$C*H*$_2$COO-, -C*H*$_2$OCO-), 2.84 (tt, 4H, -NCOC*H*$_2$C*H*$_2$CO-), 3.20 (tt, 2H, -NHC*H*$_2$CH$_2$-), 4.00 (tt, 4H, -C*H*$_2$OCO), 4.59 (tt, 1, CH$_2$C*H*CO, NH), 5.87 (t, 1H, OCN*H*CH$_2$-), 6.62 (d, 1H, OCOCHN*H*CO-). ESI-MS: [M +Na]$^+$ 1012.7.

(**5c**): 0.88 (t, 6H, -C*H*$_3$), 1.25 (m, 82H, C*H*$_2$), 1.47 (m, 2H, -NHCH$_2$C*H*$_2$CH$_2$), 1.61 (m, 6H, -C*H*$_2$CH$_2$-OCO, -C*H*$_2$CH$_2$COO-), 1.91, 2.09 (tt, 2H, -COCH$_2$C*H*$_2$CHCO, NH), 2.35 (h, 2H, -COC*H*$_2$CH$_2$-), 2.50 (tt, 2H, NHCOC*H*$_2$CH$_2$COO-), 2.55 (tt, 4H, NHCOCH$_2$C*H*$_2$COO-, -C*H*$_2$OCO-), 2.84 (tt, 4H, -NCOC*H*$_2$C*H*$_2$CO-), 3.20 (tt, 2H, -NHC*H*$_2$CH$_2$-), 4.00 (tt, 4H, -C*H*$_2$OCO), 4.59 (tt, 1, CH$_2$C*H*CO,NH), 5.87 (t, 1H, OCN*H*CH$_2$-), 6.62 (d, 1H, OCOCHN*H*CO-). ESI-MS: [M +Na]$^+$ 1069.0.

Theoretical models used to fit the SAXS data

Micelles

Considering the structure of the amphiphile, micelles were modelled as a core-multishell sphere with two shells, where the core contains the hydrophobic C_{16} dialkyl chain, shell 1 is composed of the C_2 spacer and the hydrophilic amino acid that is used to link the C_{16} chains, and shell 2 is composed by the C_{12} spacer that is used for the nanotube formation and the amino-C_6 linker of the ssDNA. Based on these assignments, the form factor P(q) for the model can be written as shown in eqn (1):

$$P(q) = \frac{scale}{V_s}[3V_c(\rho_c - \rho_{s1})\frac{[\sin(qR_c) - qR_c\cos(qR_c)]}{(qR_c)^3} + 3V_{s1}(\rho_{s1} - \rho_{s2})\frac{[\sin(qR_{s1}) - qR_{s1}\cos(qR_{s1})]}{(qR_{s1})^3} + 3V_{s2}(\rho_{s2} - \rho_{solv})\frac{[\sin(qR_{s2}) - qR_{s2}\cos(qR_{s2})]}{(qR_{s2})^3}]^2 + bkg \quad (1)$$

Where V_c, V_{s1}, V_{s2} are the volumes of the core, shell 1, and shell 2, respectively; Rc, Rs_1, Rs_2 are the radii of the core, shell 1, and shell 2; ρ_c, ρ_{s1}, ρ_{s2}, ρ_{solv} are the scattering length densities of the core, shell 1, shell 2, and the solvent; *scale* is a scale factor that equals to volume fraction when the data are on absolute scale; and *bkg* is the background level. The radii of the shells can be rewritten as a function of the thickness of each corresponding shell, as shown in eqn (2) to (3):

$$R_{s1} = R_c + t_{s1} \quad (2)$$

$$R_{s2} = R_c + t_{s1} + t_{s2} \quad (3)$$

Modelling parameters

Molecular constraints were used in the fits to reduce the number of fitting parameters. The scattering length densities were calculated based on the atomic scattering factors, molecular weights, and densities, according to eqn (4):

$$\rho_{X-ray} = \frac{\sum_i r_e Z_i}{V} \quad (4)$$

Where r_e is the classical electron radius (2.82 x 10^{-15} m), Z_i is the atomic number of the ith atom in the molecule, and V is the specific volume of the molecule. For the hydrophobic dialkyl tail, V was estimated by the density of C_{16} hydrocarbons. For the ssDNA, V can be estimated from the corresponding partial specific volume using eqn (5):[1]

$$V = \frac{\tilde{v}M_w}{N_A} \quad (5)$$

Where $\tilde{v}$ is the partial specific volume of the nucleic acid, M_w is its molecular weight and N_A is Avogadro's number. The calculated scattering length densities are presented in Table S3. Size polydispersity was also included by considering a lognormal distribution.

Nanotubes

The nanotubes were modeled as core-shell cylinders. The form factor of the cylinder can be written according to eqn (6) to (8):

$$P(q,\alpha) = \frac{scale}{V_s} f^2(q) + bkg \quad (6)$$

$$f(q) = V_c(\rho_c - \rho_s)\frac{\sin\left(q\frac{1}{2}L\cos\alpha\right)}{q\frac{1}{2}L\cos\alpha}\frac{2J_1(qR_c\sin\alpha)}{qR_c\sin\alpha} + V_s(\rho_s - \rho_{solv})\frac{\sin\left(q(\frac{1}{2}L+t_s)\cos\alpha\right)}{q(\frac{1}{2}L+t_s)\cos\alpha}\frac{2J_1(q(R_c+t_s)\sin\alpha)}{q(R_c+t_s)\sin\alpha} \quad (7)$$

$$V_s = \pi(R_c + t_s)^2 L \quad (8)$$

Where α is the angle between the axis of the cylinder and the q-vector; V_c, V_s are the volumes of the core, and shell of the cylinder, respectively; R_c is the radius of the core; ρ_c, ρ_s, ρ_{solv} are the scattering length densities of the core, shell, and the solvent; L is the cylinder length; t_s is the shell thickness; *scale* is a scale factor that equals to volume fraction when the data is on absolute scale; the *bkg* is the background level; J_1 is the first-order Bessel function. The calculated scattering length densities for the tubes are presented in Table S4. Considering it is a hollow tube, the core scattering density was set

to the same value as the solvent. The scattering length density of the shell was calculated as an average of the several layers that compose the wall of the tubes.

References

1 K. L. Sarachan, J. E. Curtis and S. Krueger, *J. Appl. Crystallogr.*, 2013, **46**, 1889-1893.

Figures

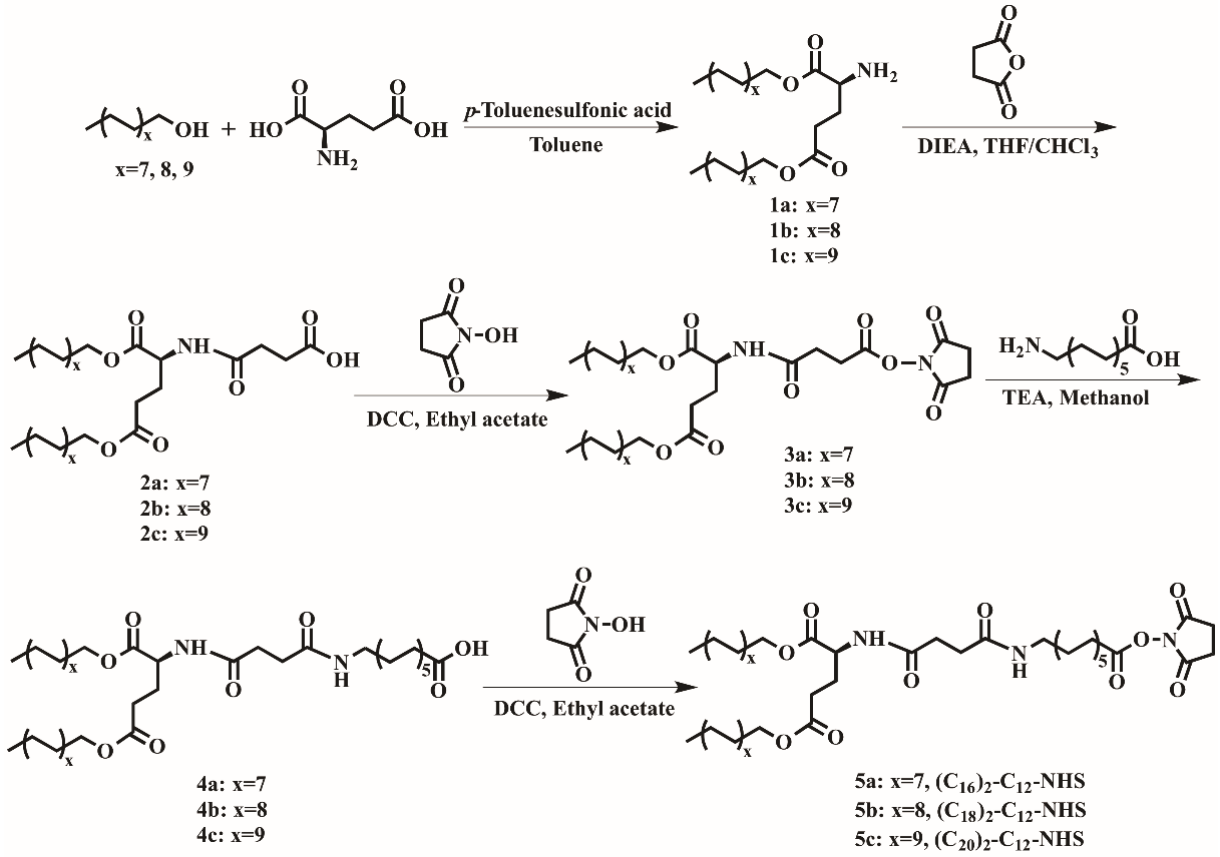

Fig. S1 Synthesis scheme of hydrophobic dialkyl tails with different lengths and a C_{12} spacer.

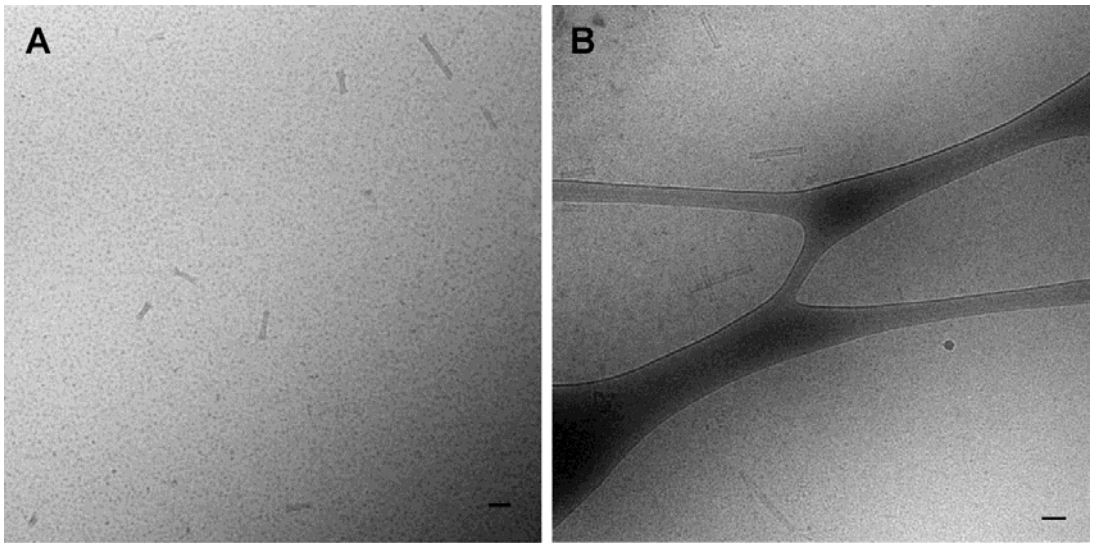

Fig. S2 Cryo-TEM images of spherical micelles and nanotubes formed by (A) 25nt-1G_8 amphiphiles, and (B) 40ntG_{12} amphiphiles, with $(C_{16})_2$ tails in water. Scale bars are 100 nm.

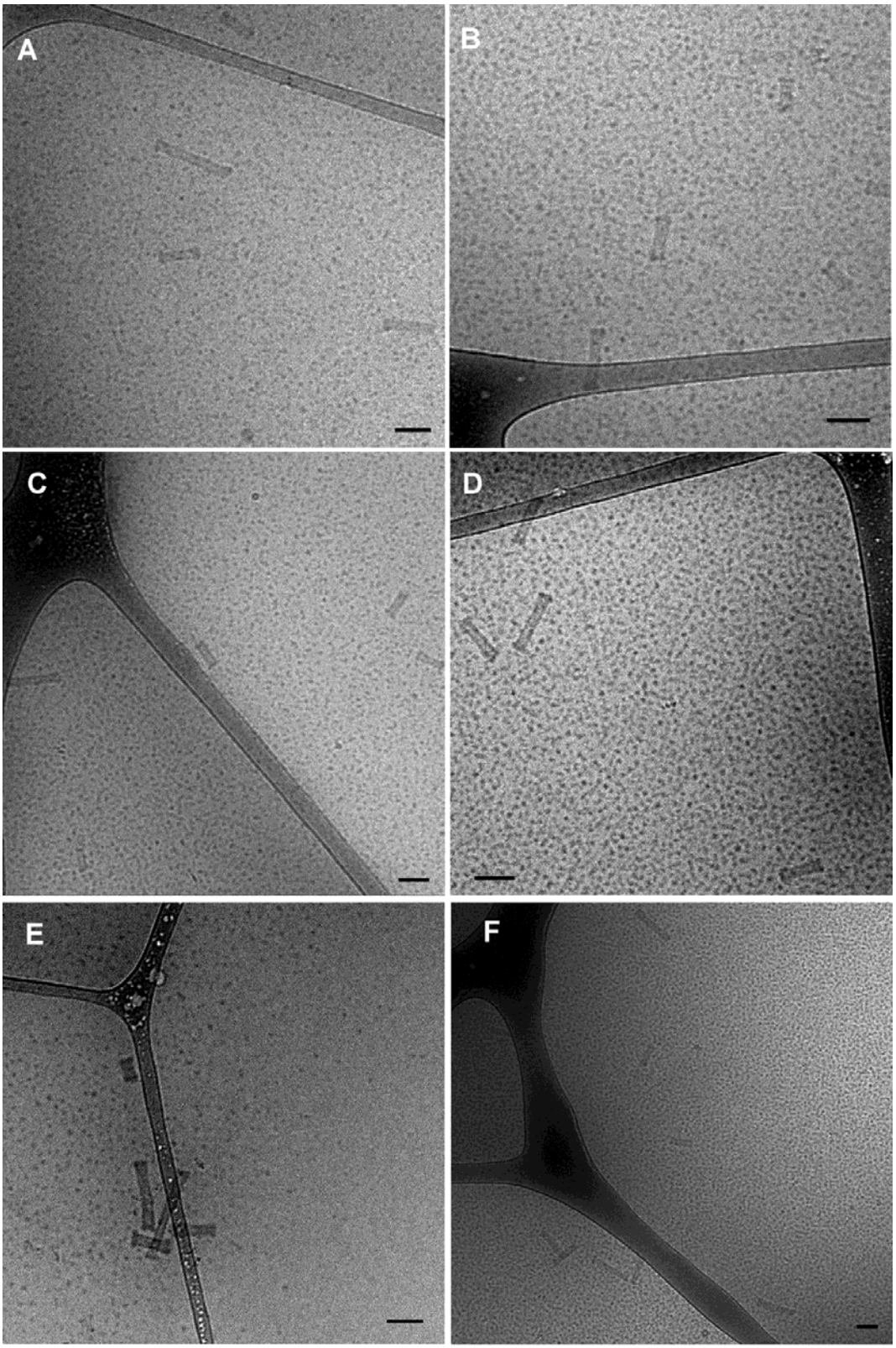

Fig. S3 Cryo-TEM images of spherical micelles and nanotubes formed by 25ntG_{12} amphiphiles with $(C_{16})_2$ tails in water and diluted overnight with (A) 100 mM KCl, (B) 100 mM NaCl, (C) 5 mM $CaCl_2$, (D) 5 mM $MgCl_2$, (E) 100 mM acetate buffer pH 5.0, (F) 100 mM carbonate-bicarbonate buffer pH 9.0. All scale bars are 100 nm.

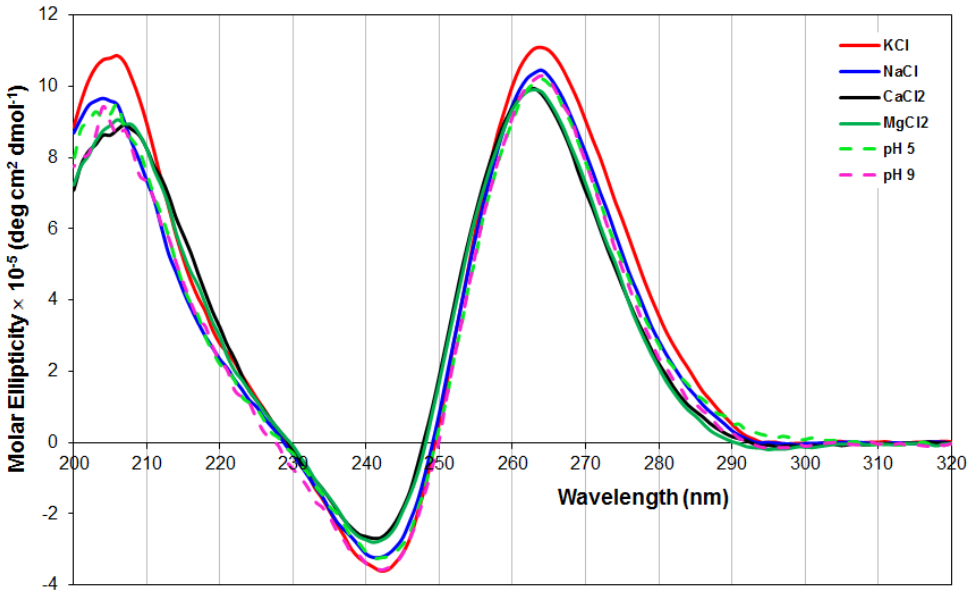

Fig. S4 CD spectra of 25ntG$_{12}$ amphiphiles with $(C_{16})_2$ tails formed in water and diluted overnight with different electrolytes (100 mM KCl, 100 mM NaCl, 5 mM $CaCl_2$, 5 mM $MgCl_2$) or buffers (100 mM acetate buffer pH 5.0, 100 mM carbonate-bicarbonate buffer pH 9.0).

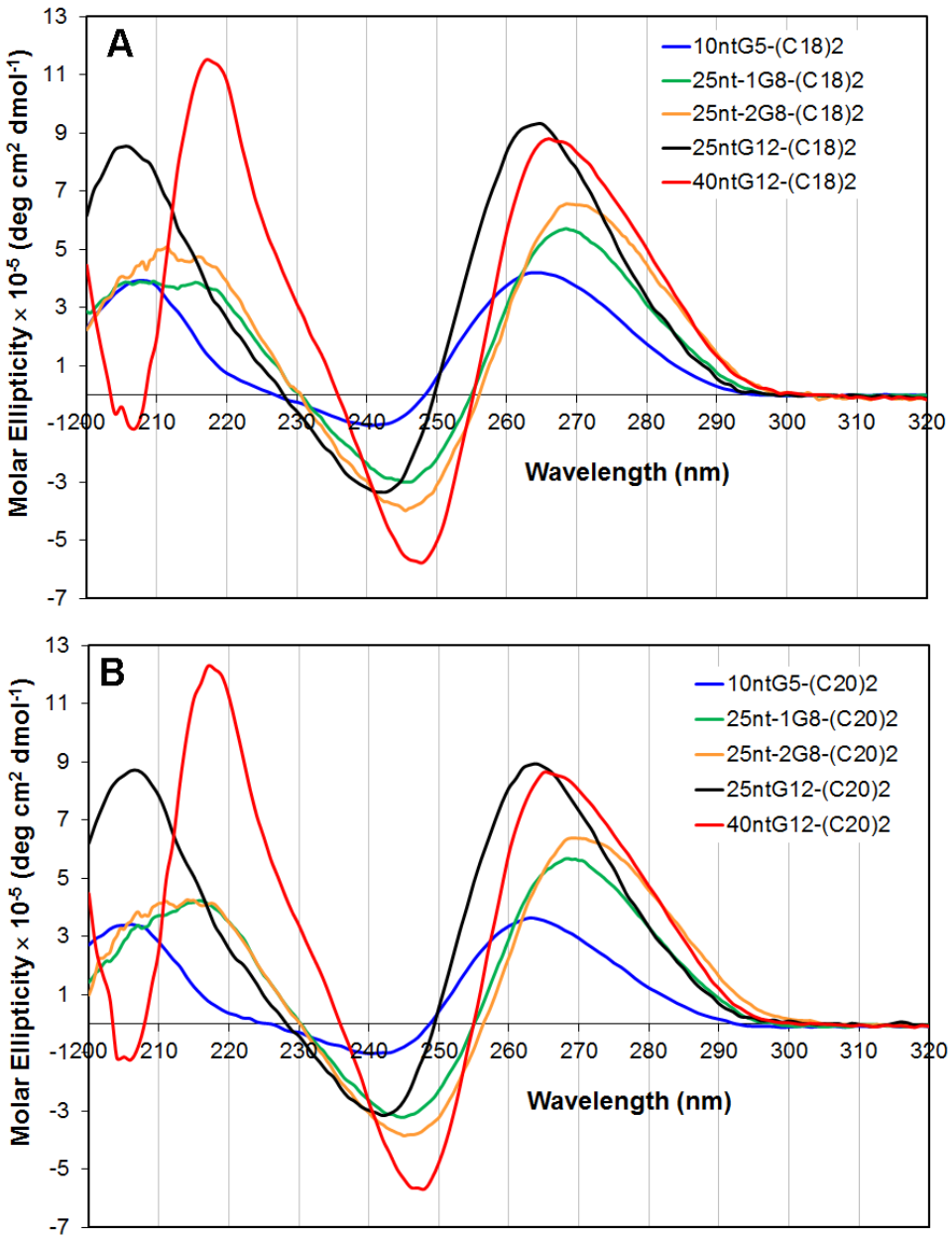

Fig. S5 CD spectra in water of G-rich ssDNA-amphiphiles with (A) $(C_{18})_2$ tails, and (B) $(C_{20})_2$ tails.

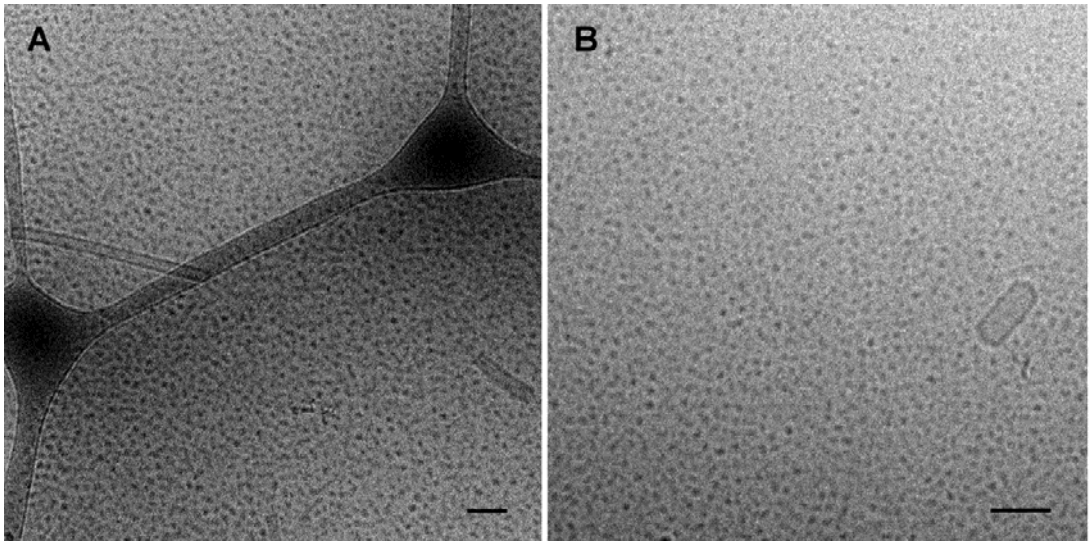

Fig. S6 Cryo-TEM images of spherical micelles and nanotubes formed by 10ntG$_5$ amphiphiles with (A) $(C_{18})_2$ tails, and (B) $(C_{20})_2$ tails in water. Scale bars are 100 nm.

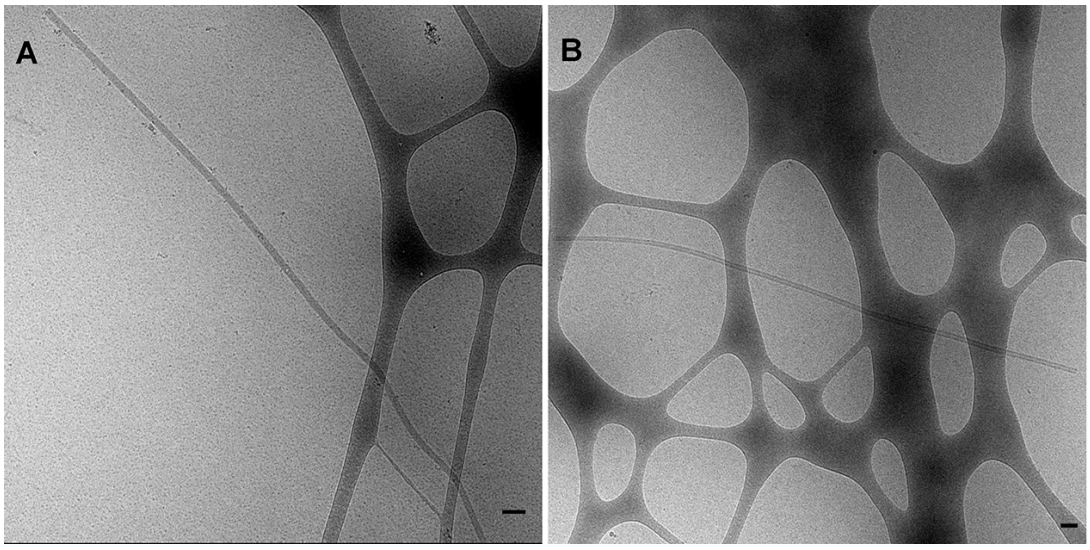

Fig. S7 Cryo-TEM images of spherical micelles and nanotubes formed by 10nt amphiphiles with no G (5'–TTCTATTCTC–3') with (A) $(C_{18})_2$ tails, and (B) $(C_{16})_2$ tails in water. Scale bars are 100 nm.

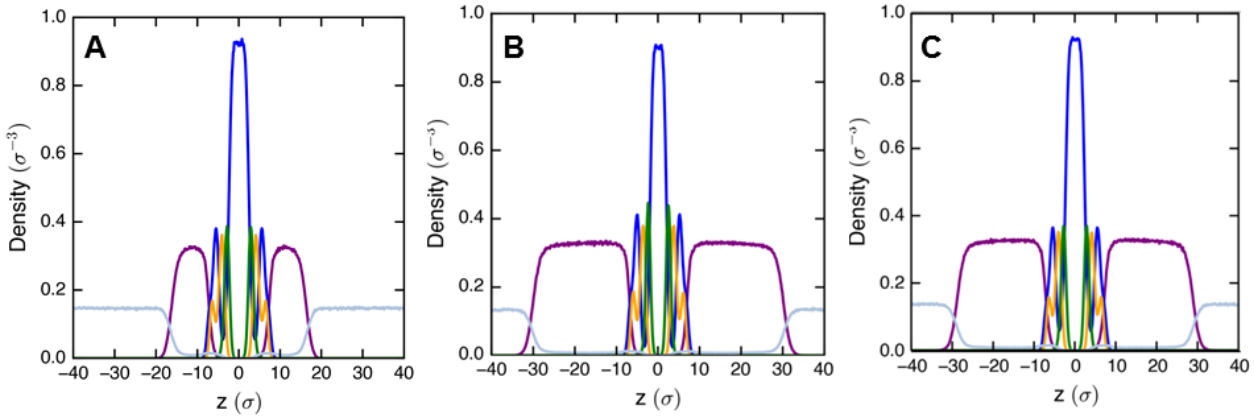

Fig. S8 Number density of various coarse-grained beads as a function of position normal to the bilayer (z) for bead types T (blue), C (green), A (orange), H (purple), and W (light blue) in the (**A**) 10nt-$(C_{20})_2$, (**B**) 25nt-$(C_{16})_2$, and (**C**) 25nt-$(C_{20})_2$ amphiphiles.

Tables

Table S1 Masses of ssDNA-amphiphiles as determined by LC-MS

ssDNA-amphiphiles	Expected mass (M-H)	Observed mass (M-H)
10ntG_5-(C_{18})$_2$	4184.9	4186.3
10ntG_5-(C_{20})$_2$	4241.8	4242.1
25nt-1G_8-(C_{16})$_2$	8803.6	8803.3
25nt-1G_8-(C_{18})$_2$	8858.9	8860.4
25nt-1G_8-(C_{20})$_2$	8915.8	8917.3
25nt-2G_8-(C_{16})$_2$	8803.6	8805.3
25nt-2G_8-(C_{18})$_2$	8858.9	8862.2
25nt-2G_8-(C_{20})$_2$	8915.8	8917.8
25ntG_{12}-(C_{16})$_2$	8894.7	8896.0
25ntG_{12}-(C_{18})$_2$	8950.0	8952.4
25ntG_{12}-(C_{20})$_2$	9006.9	9008.7
40ntG_{12}-(C_{16})$_2$	13460.6	13461.0
40ntG_{12}-(C_{18})$_2$	13515.9	13518.2
40ntG_{12}-(C_{20})$_2$	13572.8	13574.8

Table S2 Summary of non-bonded interactions in simulations

Bead type	H	T	A	C	W
H	0.75[a]	WCA[b]	WCA	WCA	0.25
T	WCA	1.5	WCA	WCA	WCA
A	WCA	WCA	0.5	WCA	WCA
C	WCA	WCA	WCA	0.5	WCA
W	0.25	WCA	WCA	WCA	0.75

[a]Numbers are ε_{ij} in the Lennard-Jones (LJ) potential for bead types *i* and *j*, reported in LJ reduced units.
[b]WCA denotes the purely-repulsive LJ potential with $\varepsilon_{ij} = 1.0$, cut and shifted at $2^{1/6}\,\sigma_{ij}$.

Table S3 Scattering length densities calculated for the core-multishell sphere

	Formula	Specific volume ($cm^3\ g^{-1}$)	ρ ($10^{10}\ cm^{-2}$)
Core	$C_{32}H_{66}$	1.28	6.63
Shell 1	$C_9H_{11}O_6N_2$	0.648	11.8
Shell 2	$C_{18}H_{35}O_1N_1$	1.28	6.63
Solvent	H_2O	1	9.43

Table S4 Scattering length densities calculated for the core-shell cylinder model

	Formula	Specific volume ($cm^3\ g^{-1}$)	ρ ($10^{10}\ cm^{-2}$)
Core	H_2O	1	9.43
Shell	Tail	0.835	13.56
Solvent	H_2O	1	9.43

Table S5 Statistical analysis comparing the lengths of nanotubes formed by G-rich amphiphiles with $(C_{16})_2$ tails in water[a]

	25nt-1G_8	25nt-2G_8	25ntG_{12}	40ntG_{12}
10ntG_5	$p>0.05$	$p>0.05$	$p<0.05$	$p<0.05$
25nt-1G_8		$p<0.05$	$p<0.05$	$p>0.05$
25nt-2G_8			$p<0.05$	$p<0.05$
25ntG_{12}				$p<0.05$

[a]p-values from one-way ANOVA with post-hoc Tukey's HSD test analysis comparing the lengths of nanotubes shown in Table 2 (n=100).

Table S6 Statistical analysis comparing the lengths of nanotubes formed by G-rich amphiphiles with $(C_{16})_2$-$(C_{20})_2$ tails in water[a]

	$(C_{18})_2$	$(C_{20})_2$	
$10ntG_5$	$p>0.05$	$p<0.05$	$(C_{16})_2$
		$p>0.05$	$(C_{18})_2$
$25nt\text{-}1G_8$	$p>0.05$	$p<0.05$	$(C_{16})_2$
		$p>0.05$	$(C_{18})_2$
$25nt\text{-}2G_8$	$p>0.05$	$p>0.05$	$(C_{16})_2$
		$p>0.05$	$(C_{18})_2$
$25ntG_{12}$	$p>0.05$	$p>0.05$	$(C_{16})_2$
		$p>0.05$	$(C_{18})_2$
$40ntG_{12}$	$p<0.05$	$p<0.05$	$(C_{16})_2$
		$p>0.05$	$(C_{18})_2$

[a]p-values from one-way ANOVA with post-hoc Tukey's HSD test analysis comparing the lengths of nanotubes shown in Table 2 and 4 (n=20).

Table S7 Statistical analysis comparing the lengths of nanotubes formed by G-rich amphiphiles with $(C_{18})_2$ tails in water[a]

$25nt\text{-}1G_8$	$25nt\text{-}2G_8$	$25ntG_{12}$	$40ntG_{12}$	
$p>0.05$	$p>0.05$	$p>0.05$	$p<0.05$	$10ntG_5$
	$p>0.05$	$p>0.05$	$p<0.05$	$25nt\text{-}1G_8$
		$p<0.05$	$p>0.05$	$25nt\text{-}2G_8$
			$p<0.05$	$25ntG_{12}$

[a]p-values from one-way ANOVA with post-hoc Tukey's HSD test analysis comparing the lengths of nanotubes shown in Table 4 (n=20).

Table S8 Statistical analysis comparing the lengths of nanotubes formed by G-rich amphiphiles with $(C_{20})_2$ tails in water[a]

25nt-1G_8	25nt-2G_8	25ntG_{12}	40ntG_{12}	
p>0.05	p>0.05	p>0.05	p<0.05	10ntG_5
	p>0.05	p>0.05	p<0.05	25nt-1G_8
		p>0.05	p<0.05	25nt-2G_8
			p<0.05	25ntG_{12}

[a]p-values from one-way ANOVA with post-hoc Tukey's HSD test analysis comparing the lengths of nanotubes shown in Table 4 (n=20).